Extended Short Multipath Insensitive Code Loop

Journal:	*IEEE Internet of Things Journal*
Manuscript ID	IoT-10230-2020.R1
Manuscript Type:	Regular Article
Date Submitted by the Author:	03-Aug-2020
Complete List of Authors:	Weng, Xu; Beihang University, ; Kou, Yanhong; Beihang University,
Keywords:	Sensor Signal Processing < Sub-Area 1: Sensors and Devices for IoT, Global Positioning System (GPS), pseudolite, indoor positioning, short multipath, S-curve, correlator, discriminator, short multipath insensitive code loop discriminator (SMICLD)

Extended Short Multipath Insensitive Code Loop

Xu Weng, Yanhong Kou

***Abstract*—Short multipath can induce large positioning errors in Global Positioning System (GPS) based high-precision location services that are vital for many applications of Internet of Things (IoT). The S-curve zero-crossing point of Short Multipath Insensitive Code Loop Discriminator (SMICLD) has no bias in the presence of single short multipath. However, when code errors turn into negative, SMICLD always outputs zero, which will cause large code errors in noise environment. In this paper, Extended Short Multipath Insensitive Code Loop (ESMICL) is proposed to resolve such deficiency by extending SMICLD's S-curve in the region where code errors are positive to the region where code errors are negative. Test results show that the lower bound of multipath delay that ESMICL can handle reaches 0.01 chips for GPS L1 C/A signals. Additionally, in the presence of single short multipath and noise, ESMICL outperforms Short Multipath Insensitive Code Loop (SMICL), Modified Delay Lock Loop Aided by SMICLD (MDAS), Narrow Correlator (NC) and Multipath Estimating Delay Lock Loop (MEDLL). In a real short multipath scene, compared with SMICL, the positioning errors of x, y and z axes of ESMICL are diminished by more than 84%, 94% and 93% respectively.**

***Index Terms*— Global Positioning System (GPS), pseudolite, indoor positioning, short multipath, S-curve, correlator, discriminator, short multipath insensitive code loop discriminator (SMICLD)**

I. Introduction

High-precision positioning based on Global Positioning System (GPS) is a significant and promising technology for Internet of Things (IoT) [1], [2], [3]. For example, it can be used to find a shared bicycle and calculate the bicycle's trajectory in city canyons [4]. It can also provide important information for Vehicular to Everything (V2X) to avoid collisions [5]. Additionally, it can be employed in indoor positioning if pseudolites are deployed in rooms [6]. However, as Fig. 1 shows, short multipath exists in these challenging positioning applications due to the limited space and will induce large positioning errors that are hard to eliminate [7], [8].

Although researchers worldwide have proposed many multipath mitigating methods [9], [10], including antenna-based [11] [12], parameter-estimation-based [13], [14], [15], [16] and correlator or discriminator-based techniques [17], [18], [19], [20], these methodologies have little effect on short multipath. The shorter the multipath delay is, the more similar the multipath is to Line of Sight (LOS) signal, which makes the receiver hard to distinguish between them. Some short multipath mitigating methods have been proposed, but they all have some limits and shortcomings.

In [21], A-Posteriori Multipath Estimation (APME) technique based on the tight relationship between multipath errors and amplitude of received signals is proposed. APME can estimate short-multipath errors by scaling the combination of correlation values with an optimization coefficient. However, the optimization coefficient is relevant to the multipath-to-direct ratio (MDR) of amplitude that is unknown to receivers. Additionally, the optimization coefficient fixed in [21] is only suitable for weak multipath with MDR below 0.25, which extremely limits APME's application. The anti-short-multipath methods proposed in [22] and [23] are similar to APME.

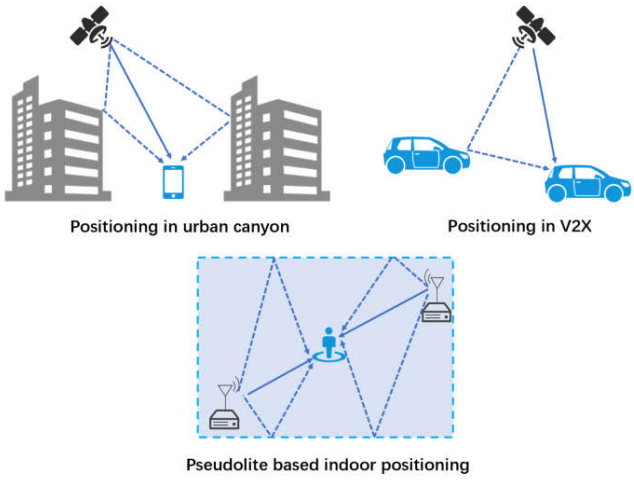

Fig. 1 Positioning Applications in Short Multipath Environment

In [24], a short multipath mitigating technique based on virtual multipath is proposed, which shares the same autocorrelation function (ACF) peak with the received signal. By subtracting the ACF values of virtual multipath from that of the received signal, the peak of the rest ACF will have no multipath bias, which corresponds to the zero code error. But the precondition that there is a multipath ray stronger than LOS and other multipath signals restricts its applications.

The authors of [25] improved the short multipath mitigation performance of Narrow Correlator (NC) [17] by using Teager-Kaiser operator that can convert the subtle changes of ACF amplitude of received signals into pulses. Thus, the multipath delay can be estimated by detecting these pulses. This method improves NC's performance on multipath with delay of less than 0.5 chips (GPS L1 C/A). However, when multipath delay reduces to 0.1 chips or less, the adjacent pulses will get too close to be detected.

Manuscript received XXXX. This work was supported in part by the National Natural Science Foundation of China (Grant No. 61271197).

Y. Kou is with the School of Electronics and Information Engineering, Beihang University, Beijing, China (e-mail: kouy@buaa.edu.cn).

X. Weng is with the School of Electronics and Information Engineering, Beihang University, Beijing, China. (e-mail: wengxu@buaa.edu.cn).

Authors of [26] proposed a multipath mitigation method based on Fast Orthogonal Search (FOS) that tries to minimize the difference between the correlation measurements and the correlation estimations, which is similar to Multipath Estimating Delay Lock Loop (MEDLL) [15], [27], [28]. Even superior to MEDLL and NC, this FOS-based technique still has larger code errors for short multipath than medium and long multipath. Moreover, FOS requires heavy computational loads, which is high demanding for receiver hardware.

Short Multipath Insensitive Code Loop Discriminator (SMICLD) introduced in [29] modifies correlation values and the code discriminator so that the zero-crossing point of its discriminator curve (S-curve) has no bias in short multipath environment. However, when code errors are negative, SMICLD always outputs zero, which results in ambiguous distinction between negative and zero code errors. As a result, SMICLD is sensitive to noise seriously. Modified Short Multipath Insensitive Code Loop Discriminator (MSMICLD) proposed in [30] and New Modified Short Multipath Insensitive Code Loop Discriminator (New MSMICLD) proposed in [31] are respectively the non-coherent envelope and non-coherent dot product power versions of SMICLD. The code loop using SMICLD as its discriminator is called Short Multipath Insensitive Code Loop (SMICL).

Modified Delay Lock Loop Aided by SMICLD (MDAS) proposed in [32] and [33] has improved the S-curve of SMICLD. The algorithm uses SMICLD for positive and zero code errors, and switches to the modified early minus late discriminator (MEMLD) for negative code errors. And a correlation channel that is later than the prompt correlation channel is added to switch the code loop to the proper discriminator [34]. This code loop integrates the advantages of SMICLD and MEMLD, which can not only mitigate short multipath but also adjust negative code errors promptly. However, there's a large gap at the zero-crossing point of the S-curve of MDAS, which degrades its multipath mitigating performance when noise exists.

In order to improve the S-curve of SMICLD and its short multipath mitigation in noise environment, key contributions in this paper are summarized as follows.

- We design Extended Short Multipath Insensitive Code Loop (ESMICL) by extending SMICLD's S-curve in the region where code errors are positive to the region where code errors are negative. It mainly consists of three sections: SMICLD, MEMLD and multi-correlators. The multi-correlator module is used to estimate code errors, which is the key to extending the S-curve of SMICLD.
- ESMICL is implemented in our software-defined GPS L1 C/A Intermediate Frequency (IF) receiver. Its short multipath mitigating performance and anti-noise ability are compared not only with SMICL and MDAS, but also with conventional code loops including NC and MEDLL by using the digital IF GPS signal simulator in the following aspects.
  1. The code errors in time domain.
  2. The mean and standard deviation of code errors with respect to different carrier to noise ratio (C/N0).
  3. The multipath code error envelope.
  4. The positioning errors.

Test results indicate that ESMICL has the best single short multipath mitigation performance in noise environment among above code loops.

The paper is organized as follows. Section II and III give a brief description of the short multipath model and the assessment of SMICLD, respectively. Section IV illustrates the principles of ESMICL in detail. Test results and comparative analysis will be displayed in Section V. Finally, Section VI summarizes this study and makes some suggestions for future research.

TABLE I
LIST OF THE KEY ACRONYMS AND ABBREVIATION

C/N0	Carrier to Noise Ratio
DLL	Delay Lock Loop
EMLD	Early Minus Late Discriminator
ESMICL	Extended Short Multipath Insensitive Code Loop
ESMICLD	Extended Short Multipath Insensitive Code Loop Discriminator
GPS	Global Positioning System
IF	Intermediate Frequency
LOS	Line of Sight
MDR	Multipath-to-Direct Ratio
MEDLL	Multipath Estimating Delay Lock Loop
MEMLD	Modified Early minus Late Discriminator
MDAS	Modified Delay Lock Loop Aided by SMICLD
MoSMICLD	Discriminator of MDAS
NC	Narrow Correlator
NC-EMLD	Narrow Correlator Early Minus Late Discriminator
NCO	Numerically Controlled Oscillator
RF	Radio Frequency
S-curve	Discriminator Curve
SMICL	Short Multipath Insensitive Code Loop
SMICLD	Short Multipath Insensitive Code Loop Discriminator

TABLE II
LIST OF THE KEY SYMBOLS

a_0	Amplitude of LOS Signal
τ_0	Propagation Time of LOS Signal
θ_0	Carrier Phase of LOS Signal
a_i	Amplitude of the i^{th} Multipath
τ_i	the i^{th} Multipath Delay Relative to LOS Signal
θ_i	Carrier Phase of the i^{th} Multipath
$d\theta_i$	Carrier Phase Difference between LOS and the i^{th} Multipath
τ	Code Phase of Local Replica
M	Number of Multipath Signals
ε	Code Error
w	Carrier Frequency
Δ_m	Correlator Spacing of MEMLD
Δ, Δ_{SMICLD}	Correlator Spacing of SMICLD
$\Delta_{MoSMICLD}$	Correlator Spacing of SMICLD in MDAS
$\Delta_{ESMICLD}$	Correlator Spacing of SMICLD in ESMICL
Δ_{NC}	Correlator Spacing of EMLD in NC
Δ_{MEDLL}	Correlator Spacing of EMLD in MEDLL
$p(t)$	C/A Code Sequence
$D(t)$	Navigation Message Data
D_d^{max}	Maximum Value of SMICLD in the Interval of [0 d]
f_s	Sampling Frequency
f_{IF}	Intermediate Frequency
IP	In-phase Prompt Correlation Value
QP	Quadrature Prompt Correlation Value
IE	In-phase Early Correlation Value
QE	Quadrature Early Correlation Value
IL	In-phase Late Correlation Value
QL	Quadrature Late Correlation Value
IF	In-phase Forward Correlation Value
QF	Quadrature Forward Correlation Value

II. Short Multipath Model

The GPS L1 C/A IF signal distorted by multipath can be expressed as [35]

$$r(t) = a_0 p(t - \tau_0) D(t - \tau_0)\cos(wt + \theta_0) + \sum_{i=1}^{M} a_i p(t - \tau_0 - \tau_i) D(t - \tau_0 - \tau_i)\cos(wt + \theta_i) \quad (1)$$

If the signal expressed by (1) is normalized by the LOS signal, a_i will denote MDR.

There is no definite standard for short multipath. Some researchers consider the delay of short multipath is less than 1chip or 0.5 chips, which depends on the specific positioning scenarios. In this paper, the multipath with delay of less than 0.1 chips (about 30 m for GPS L1 C/A signal) will be focused on.

In the receiver, the replica C/A code is represented by $p(t-\tau)$, which is delayed by τ relative to the direct signal. θ is the carrier phase of local carrier. After carrier wipe-off and code correlation process, the in-phase prompt correlation value IP can be written as

$$IP = a_0 R(\varepsilon)\cos(\theta_0 - \theta) + \sum_{i=1}^{M} a_i R(\varepsilon - \tau_i)\cos(\theta_i - \theta) \quad (2)$$

In (2), it is assumed that the data sequence doesn't transition during the integration time, so $D(t)$ can be neglected. The code error ε is the code phase difference between the LOS signal and the local replica.

$$\varepsilon = \tau - \tau_0 \quad (3)$$

Theoretically, a triangle function is usually used as the autocorrelation function $R(\varepsilon)$ of C/A codes [36].

$$R(\varepsilon) = \begin{cases} 1 - |\varepsilon| & , |\varepsilon| \le 1 \text{ chip} \\ 0 & , \text{others} \end{cases} \quad (4)$$

III. Assessment of Short Multipath Insensitive Code Loop Discriminator (SMICLD)

Like (2), let us denote the other quadrature prompt, in-phase early, quadrature early, in-phase late, quadrature late correlation values as QP, IE, QE, IL, QL, respectively.

The SMICLD is defined in (5), where IP' and QP' are defined as the modified prompt correlation values by (6) and (7). Δ denotes the correlator spacing.

$$D = (IE^2 + QE^2) - ((IP')^2 + (QP')^2) \quad (5)$$

$$IP' = IP - \frac{\Delta}{2}\frac{IE + IL}{2 - \Delta} \quad (6)$$

$$QP' = QP - \frac{\Delta}{2}\frac{QE + QL}{2 - \Delta} \quad (7)$$

Combined with (4), the discriminator function can be written as follows.

If $0<\tau_1<\varepsilon\le\min(\Delta/2, 1-\Delta/2)$,

$$D_{SMICLD} = 2(2 - \Delta)\left[\begin{array}{l} a_0^2\varepsilon + a_1^2(\varepsilon - \tau_1) \\ +a_0 a_1 \cos(\theta_0 - \theta_1)(2\varepsilon - \tau_1) \end{array}\right] \quad (8)$$

If $0 <\varepsilon<\tau_1\le\min(\Delta/2, 1-\Delta/2)$,

$$D_{SMICLD} = 2a_0^2(2 - \Delta)\varepsilon + 4a_0 a_1 \cos(\theta_0 - \theta_1)\varepsilon(1 + \varepsilon - \tau_1 - \frac{\Delta}{2}) \quad (9)$$

If $\tau_1 - \min(\Delta/2, 1-\Delta/2)<\varepsilon<0 <\tau_1\le\min(\Delta/2, 1-\Delta/2)$,

$$D_{SMICLD} = 0 \quad (10)$$

The assessments of SMICLD in single short multipath environment have been illustrated in TABLE III, the details of which can be found in [32].

TABLE III
SMICLD's Outputs of Different Code Error

Code Error ε	SMICLD's Output D
$\tau_1 - \min(\frac{\Delta}{2}, 1-\frac{\Delta}{2}) < \varepsilon \le 0 < \tau_1 \le \min(\frac{\Delta}{2}, 1-\frac{\Delta}{2})$	$D = 0$
$0 < \varepsilon \le \tau_1 \le \min(\frac{\Delta}{2}, 1-\frac{\Delta}{2})$	$D > 0$
$0 < \tau_1 < \varepsilon \le \min(\frac{\Delta}{2}, 1-\frac{\Delta}{2})$	$D > 0$

As TABLE III shows, when single short multipath exists, SMICLD can adjust code error from positive to zero without any bias. However, when the code error becomes negative (no less than τ_1-min ($\Delta/2$, 1-$\Delta/2$)), SMICLD outputs zero constantly, which leaves the code error without any adjustment. Such zero output seriously restricts SMICLD's application, especially in noise environment.

IV. Extended Short Multipath Insensitive Code Loop

To solve the problem that SMICLD outputs zero for negative code errors in the presence of single short multipath, Extended Short Multipath Insensitive Code Loop (ESMICL) is proposed in this section.

A. Architecture of ESMICL

Considering SMICLD can adjust code errors from positive values to zero, ESMICL is designed to extend SMICLD's S-curve in the first quadrant of εD-plane, where code errors are positive, to the third quadrant where code errors are negative. Its architecture is illustrated by the block diagram in Fig. 2.

As shown in Fig. 2, ESMICL mainly consists of three sections: MEMLD (the red section), SMICLD (the purple section) and the multi-correlator module (the blue section). Initially, the code loop discriminator is set to SMICLD. If the output of SMICLD is positive, the code error will be considered as positive correspondingly. Thus, SMICLD will continue to be used. If SMICLD outputs zero, the code error might be zero or negative. In this case, the multi-correlator module is activated to estimate the current code error, whereby the extension of SMICLD or MEMLD will be utilized.

B. Code Error Estimation

The estimation of code errors is the key to the extension of SMICLD. Let CP, n and d respectively represent the current values of the replica code phase, the number of correlation channels and the spacing between adjacent correlators in the multi-correlator module.

The code phase of the k^{th} correlator in the multi-correlator module falls behind the prompt correlator by kd, which increases the code error of the k^{th} correlator to $\varepsilon + kd$. The correlation values in the k^{th} channel are represented by IE_d^k, QE_d^k, IL_d^k, QL_d^k, IP_d^k, QP_d^k, $IP_d'^k$, $QP_d'^k$. All correlation values in the

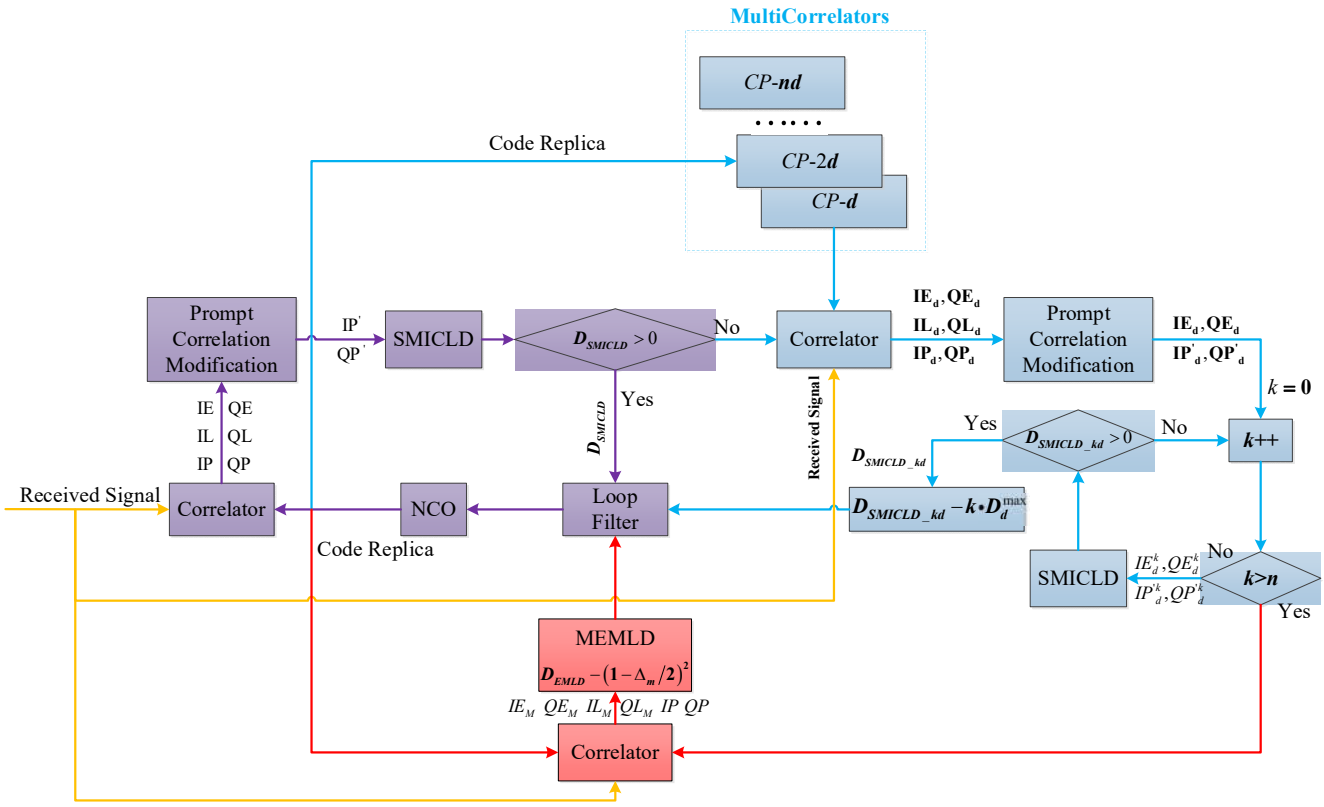

Fig. 2 Block Diagram of ESMICL

multi-correlator module can be written in the form of vectors: $\mathbf{IE}_d$, $\mathbf{QE}_d$, $\mathbf{IL}_d$, $\mathbf{QL}_d$, $\mathbf{IP}_d$, $\mathbf{QP}_d$, $\mathbf{IP}'_d$, $\mathbf{QP}'_d$.

As soon as the multi-correlator module is activated, SMICLD will be firstly updated by the correlation values of the 1st channel. If the output of SMICLD (D_{SMICLD_d}) is positive at this time, the code error ε will be in [$-d$ 0]. However, if SMICLD still outputs zero, which means the code error ε is less than $-d$, the correlation values of the 2nd correlator will be used to update SMICLD. Such operations will be repeated until SMICLD outputs a positive value. Assuming the k^{th} channel meets above requirements ($D_{SMICLD\_kd}>0$), we can determine that the code error ε is located in the interval of [$-kd$, $-(k-1)d$] (k is a positive integer and no more than n). If SMICLD still outputs zero in terms of the n^{st} channel, the code error ε will be less than $-nd$.

C. Extension of SMICLD

The discriminator of ESMICL is called Extended Short Multipath Insensitive Code Loop Discriminator (ESMICLD), which is composed of three kinds of discriminators.

If it is determined that the code error is located in the interval of [$-kd$, $-(k-1)d$], the following discrimination values will be used.

$$D_{ESMICLD} = D_{SMICLD}(\varepsilon + kd) - k \cdot D_d^{max} \tag{11}$$

D_d^{max} represents the maximum value of SMICLD in the interval of [0 d]. As illustrated in Fig. 2, when the code error ε lies in the interval of [$-kd$, $-(k-1)d$], the code error of k^{th} correlation channel $\varepsilon+kd$ must be located in the interval of [0 d]. Therefore, the output of SMICLD $D_{SMICLD}(\varepsilon+kd)$ is less than D_d^{max}. Moreover, in order to guarantee the monotonic increase of the S-curve, D_d^{max} is multipled by k and then subtracted from $D_{SMICLD}(\varepsilon+kd)$. Thus, the discriminating result $D_{ESMICLD}$ is negative and then diminishes the replica code phase. As a result, the code loop will converge to the right direction.

The process of extension of SMICLD, as illustrated by green arrows in Fig. 3, can be described as moving the S-curve of SMICLD in the interval of [0 d] to the left by kd and then downwards by kD_d^{max} to extend the positive part of the S-curve of SMICLD to the third quadrant.

If the multipath delay τ_1 is great than d, we can get the expression of D_d^{max}:

$$D_d^{max} = 4d(2 - \Delta) \tag{12}$$

The details of calculating the maximum discriminating value D_d^{max} can be referred to Appendix.

As Fig. 3 shows, there is a subtle gap at the zero-crossing point of the S-curve of ESMICL. The smaller the correlator spacing d is, the smaller the maximum value of SMICLD and this gap are. Nevertheless, the computational complexity will intensify with the increase of correlators that is the result of decreasing d. Taking into account the smaller gap at the zero-crossing point and the computational complexity, we choose six correlators spaced successively by d=Δ/64 to extend the positive S-curve of SMICLD to the region where code errors are [-6Δ/64 0] (approximately [-0.1 0] chips with Δ=1 chip). In this way, ESMICL can mitigate the short multipath with the delay of larger than Δ/64 (approximately 0.015 chips with Δ=1 chip). According to (12), the maximum discriminating value of SMICLD in the interval of [0 Δ/64] can be calculated:

$$D_{d=\Delta/64}^{max} = (2\text{-}\Delta)\bullet\frac{\Delta}{16} \quad (13)$$

It can be seen from equation (13) that the maximum gap at the zero-crossing point of ESMICLD's S-curve is $-D_d^{max}$ (about -0.06 chips with d=Δ/64 and Δ=1), much less than that of MDAS according to [32].

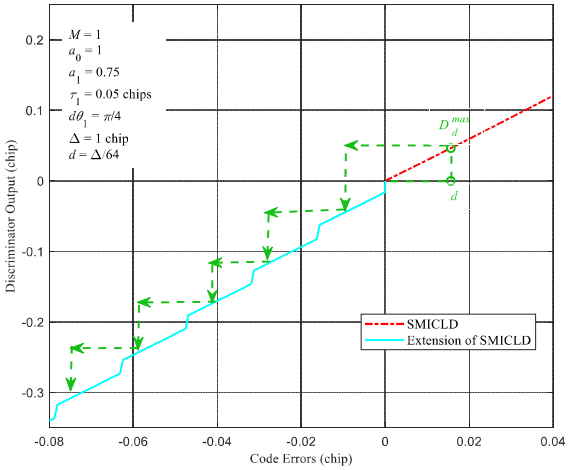

Fig. 3 Extension of SMICLD

If SMICLD still outputs zero until the *n*th correlation channel, MEMLD will be activated.

$$D_{ESMICLD} = D_{MEMLD}(\varepsilon) = D_{EMLD}(\varepsilon) - \left(1 - \frac{\Delta_m}{2}\right)^2 \quad (14)$$

Δ_m is the correlation spacing of MEMLD, which is set to 1.5Δ. To conclude, the algorithm exhibited in Table III will be used in ESMICL.

TABLE III
DISCRIMINATING ALGORITHM OF ESMICL

- If $D_{SMICLD}(\varepsilon) \geq 0$, which means the code error is positive, the code loop will continue using SMICLD
$$D_{ESMICLD} = D_{SMICLD}(\varepsilon)$$
- If $D_{SMICLD}(\varepsilon+(k\text{-}1)\Delta/64) \leq 0$ & $D_{SMICLD}(\varepsilon+k\Delta/64) \geq 0$, which means the code error is located in $[-kd\ -(k\text{-}1)d]$, the expression of Extended SMICLD is
$$D_{E\_SMICLD} = D_{SMICLD}(\varepsilon + k\bullet\Delta/64) - k\bullet(2\text{-}\Delta)\bullet\frac{\Delta}{16}$$
- If $D_{SMICLD}(\varepsilon+6\Delta/64) \leq 0$, which means the code error is less than -6Δ/64 chip, MEMLD will be used.
$$D_{ESMICLD} = D_{MEMLD}(\varepsilon)$$

D. S-curve of ESMICLD

As shown in Fig. 4, the S-curve of ESMICLD consists of three sections: the positive part of the S-curve of SMICLD ($\varepsilon \geq 0$), the negative part of the S-curve of MEMLD (where $\varepsilon < -6\Delta/64$) and the extension of the S-curve of SMICLD near the zero-crossing point (where $-6\Delta/64 < \varepsilon < 0$). $d\theta_1$ represents the difference between the carrier phase of the direct and LOS signal.

ESMICLD's S-curve is compared with those of NC-EMLD, SMICLD and MoSMICLD, which are the discriminators of NC, SMICL and MDAS, respectively. The related parameters are shown in Fig. 5.

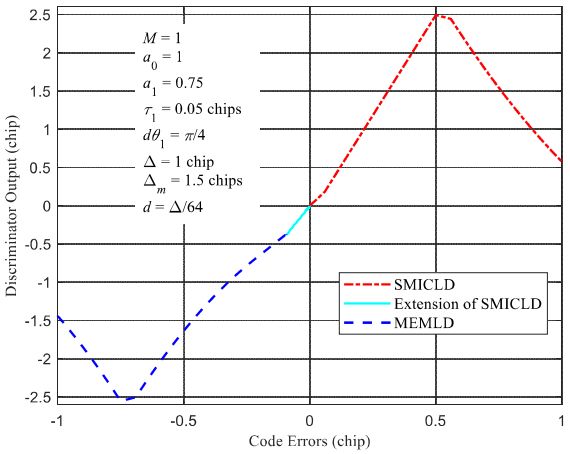

Fig. 4 S-curve of ESMICLD

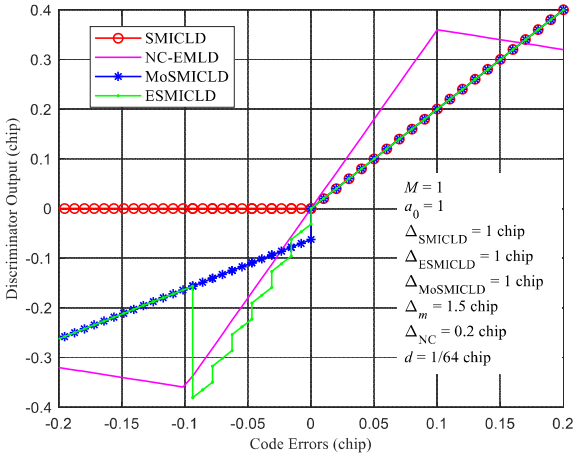

(a)

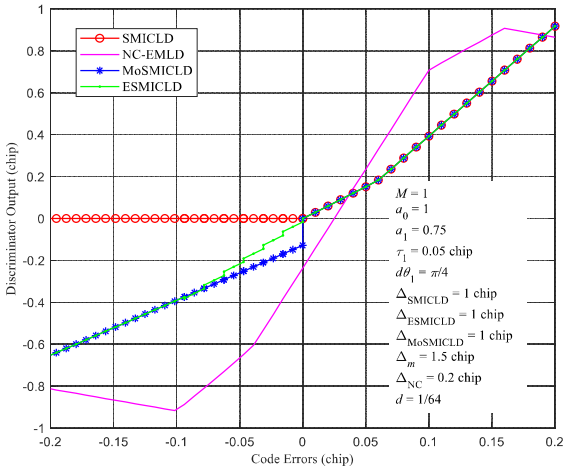

(b)

Fig. 5 S-curves of SMICLD, MoSMICLD, ESMICLD and NC-EMLD (a) without multipath and (b) with single multipath

Fig.5 (a) shows that, in an ideal multipath-free scene, both ESMICLD and MoSMICLD can discriminate negative code errors, while SMICLD cannot. However, the S-curves of ESMICLD and MoSMICLD have gaps at the zero point,

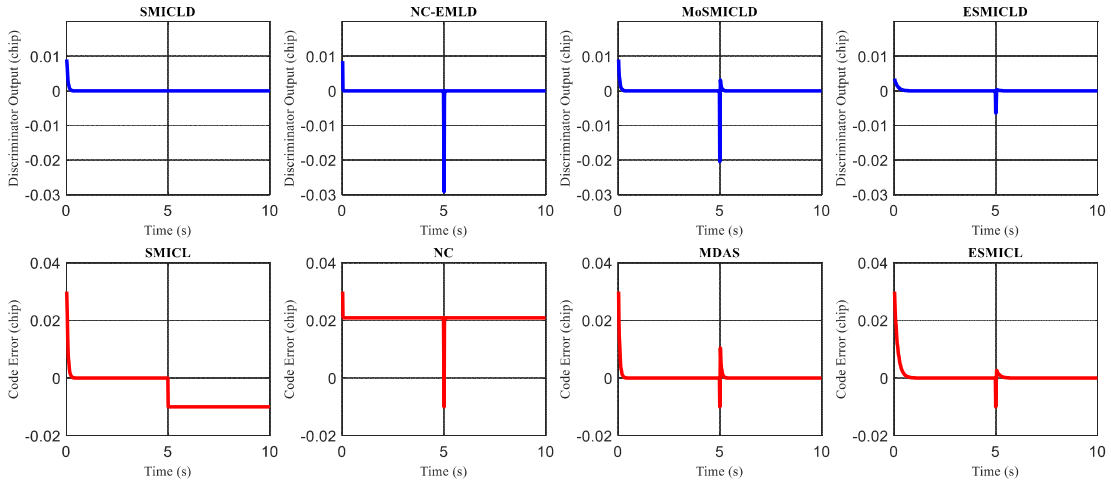

Fig. 6 Discriminator outputs and code errors of SMICL, NC-DLL, MDAS and ESMICL

which may degrade their anti-noise performance to some extent, as discussed in Section V.

As Fig. 5(b) illustrates, compared with NC-EMLD, the S-curve of ESMICLD has no bias at its zero-crossing point. Compared with SMICLD, ESMICLD outputs negative discrimination values for negative code errors. Compared with MoSMICLD, ESMICLD has a much smaller gap at the zero-crossing point of its S-curve.

A converging process of code errors in four code loops that contains above four discriminators has been simulated in Fig. 6, and the multipath and code loop parameters stay the same as those in Fig. 5. An initial code error of 0.03 chips and an abrupt code error change of -0.01 chips at the 5th second are set. This sudden code error change is used to simply simulate the interference from noise or signal blocking, which should be a gradually changing process in real circumstances.

Fig. 6 shows that the initial positive code error prompts positive output of the discriminators in the four loops to adjust replica code. Before the 5th second, the code error of NC converges to a nonzero value, a bias caused by short multipath. By contrast, the other three code loops can mitigate this kind of bias. At the 5th second, SMICLD produces zero when the code error turns into negative value, which leaves the replica code exceeding the LOS signal by 0.01 chips. In contrast, NC can respond to the abrupt mutation and pull the code error back with the same bias as before. MDAS and ESMICL can timely rectify the negative error without any bias. However, MoSMICLD has a large gap at the zero-crossing point of its S-curve, which adjusts the code error towards positive direction excessively. As a result, a positive pulse of its code error appears at about the 5th second. In comparison, ESMICLD has a much smaller gap at the zero-crossing point to adjust the replica code more temperately.

E. Normalization of ESMICLD

The above discussion about ESMICLD assumes that the received signal (1) is normalized by the amplitude of the LOS component. Indeed, in practice, such normalization must be done to deal with different power of received signals. Firstly, SMICLD is normalized according to the following equation.

$$D_{SMICLD} = \frac{(IE^2 + QE^2) - ((IP')^2 + (QP')^2)}{(IE^2 + QE^2) + (IL^2 + QL^2)} \tag{15}$$

MEMLD is normalized as follows, the details of which can be found in [33].

$$D_{MEMLD} = D_{norEMLD} - \frac{2 - \Delta_m}{\sqrt{2\left[1 + (1 - \Delta_m / 2)^2\right]} + 2 - \Delta_m / 2} \tag{16}$$

Where $D_{norEMLD}$ is

$$D_{norEMLD} = \frac{\left(IE^2 + QE^2\right) - \left(IL^2 + QL^2\right)}{\left(IE^2 + QE^2\right) + \left(IP^2 + QP^2\right)} \tag{17}$$

The normalization of ESMICLD is implemented with the help of the forward correlation channel. If the code error is estimated in the interval of [-kd, -(k-1)d], the code phase of the forward correlation channel will be greater than that of the k^{th} channel by 1 chip. In this case, the correlation values of the forward correlation channel are not interfered by the short multipath ray. The correlation values of the forward correlation channel are shown as follows.

$$\begin{aligned} IF &= a_0 R(\varepsilon + k \bullet \Delta/64 - 1)\cos(\theta_0 - \theta) \\ QF &= a_0 R(\varepsilon + k \bullet \Delta/64 - 1)\sin(\theta_0 - \theta) \\ \varepsilon &\in \left[-kd, -(k-1)d\right] \end{aligned} \tag{18}$$

Additionally, the forward late correlation channel, delayed by d_f relative to the forward correlation channel, is utilized to calculate the amplitude of the direct signal. The correlation values of the forward late correlation channel are given as follows.

$$\begin{aligned} IF_d &= a_0 R(\varepsilon + k \bullet \Delta/64 - 1 + d_f)\cos(\theta_0 - \theta) \\ QF_d &= a_0 R(\varepsilon + k \bullet \Delta/64 - 1 + d_f)\sin(\theta_0 - \theta) \\ \varepsilon &\in \left[-kd, -(k-1)d\right] \end{aligned} \tag{19}$$

To obtain the pure amplitude of the direct signal without interfered by the multipath ray, the value of d_f should be as small as possible. In this paper,

$$d_f = \frac{d}{2} = \frac{\Delta}{128} \tag{20}$$

Thus, ESMICLD is normalized as follows.

$$D_{norESMICLD} = \frac{D_{SMICLD}\left(\varepsilon + k\bullet\Delta/64\right)}{\left[\left(IF_d - IF\right)^2 + \left(QF_d - QF\right)^2\right]/d_f^2} - k\bullet(2\text{-}\Delta)\bullet\frac{\Delta}{16} \quad (21)$$

V. Experimental Results

In this section, the proposed ESMICL is compared with NC, MEDLL, SMICL and MDAS, in terms of means and standard deviations of code errors, which are employed to assess the bias induced by multipath and the fluctuation caused by noise respectively. All these code loops have been implemented in the software-defined GPS L1 C/A IF receiver developed by our groups at Beihang University. The software-defined GPS L1 C/A signal simulator developed by us are also used in the following experiments. The front-end bandwidth is not considered as its influence on the code loop is a fixed bias of code errors which can be calibrated in advance according to [29].

A. Code Errors in Short Multipath Environment

To compare the short multipath mitigation performance of NC, MEDLL, SMICL, MDAS and ESMICL in the time domain, their code errors are shown in Fig. 7(a). The parameters used in the simulation are exhibited in TABLE IV. The boxplots are exploited to analyze the distribution of code errors of the five loops, which is exhibited in Fig. 7 (b). For a quantitative comparison, means and standard deviations of code errors are summarized in TABLE V

TABLE IV
Relevant Parameters Used in the Simulation

Parameters	Values
a_1	0.6
τ_1	0.05 chips
$d\theta_1$	0.75π
f_s	100 MHz
f_{IF}	1.405 MHz
C/N0	45 dB•Hz
Δ_{SMICLD}	1 chip
$\Delta_{MoSMICLD}$	1 chip
Δ_m	1.5 chips
$\Delta_{ESMICLD}$	1 chip
Δ_{NC}	0.2 chips
Δ_{MEDLL}	0.2 chips
d	$\Delta_{ESMICLD}$ /64

Fig. 7 (a) shows that the code error of SMICL fluctuates seriously towards negative values due to noise and the zero output for negative code errors. In contrast, ESMICL and MDAS have better anti-noise ability owing to their negative output for negative code errors.

TABLE V shows that, compared with MDAS, the mean of the code error of ESMICL is diminished by an order of magnitude. Compared with NC, MEDLL and SMICL, ESMICL has diminished the code error (absolute value) by more than two orders of magnitude.

TABLE V and Fig. 7 (b) shows that the code error of ESMICL has a smaller standard deviation and distributes around zero more evenly. However, NC has the smallest standard deviation, which means it has the best anti-noise ability among all the five code loops.

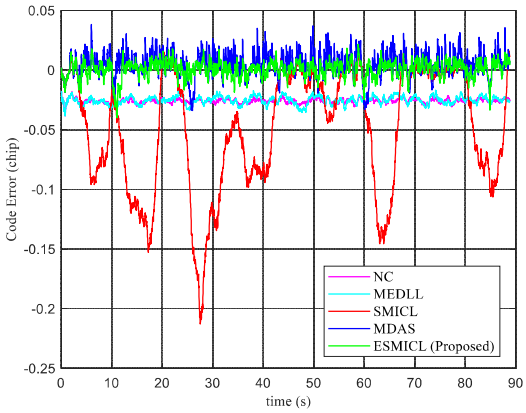

(a)

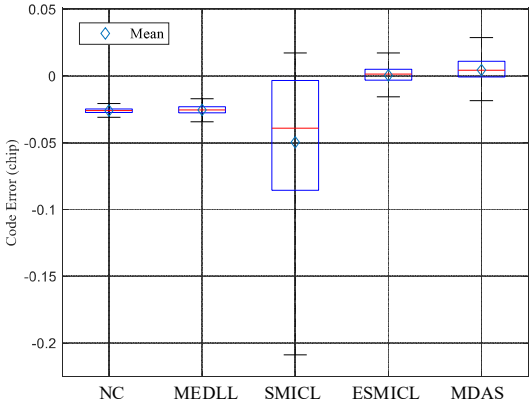

(b)

Fig. 7 (a) Code errors and (b) their boxplots of NC, MEDLL, SMICL, MDAS and ESMICL

TABLE V
Means and Standard Deviations of Code Errors

Multipath Mitigation Methods	Code errors	
	Mean (chip)	Standard Deviation (chip)
NC	-0.0260	0.0019
MEDLL	-0.0254	0.0034
SMICL	-0.0501	0.0504
MDAS	0.0044	0.0101
ESMICL	4.0917e-4	0.0071

B. Noise Performance

Fig. 8 illustrates the means and standard deviations of code errors, as well as measured C/N0 of NC, MEDLL, SMICL, MDAS and ESMICL in noise environments with different C/N0. Other parameters are the same as those in Fig. 7.

Fig. 8 displays that SMICL possesses large code error means and standard deviations. With the rise of C/N0, however, the code error of SMICL becomes smaller and smaller. It is the higher C/N0—the weaker noise—that allows the code error to lock to zero stably without drafting to the negative value. Thus, if there is no noise, MDAS and ESMICL will degrade to single SMICL.

Fig. 8 shows that ESMICL limits its code error means to 10^{-4} orders of magnitude in diverse noise background. The

anti-noise ability of ESMICL is superior to that of SMICL and MDAS. Additionally, even though NC and MEDLL can track the code phase of the received signal more stably, their code errors both have certain biases. Thus, considering that the variation can be eliminated by data processing while the bias is hard to mitigate, ESMICL is the best choice among the five code loops.

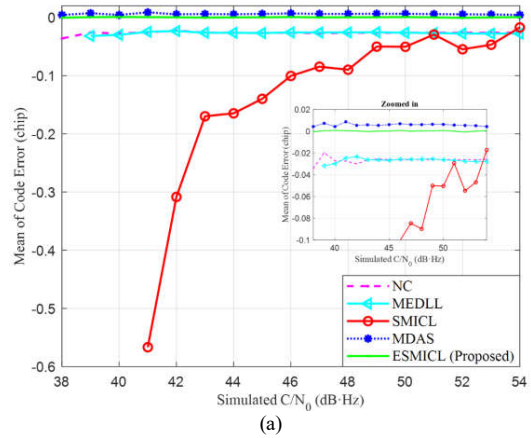

(a)

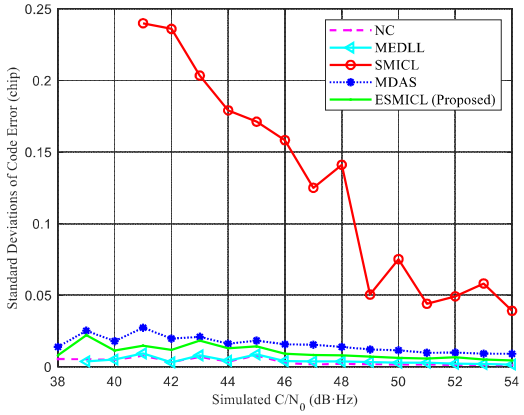

(b)

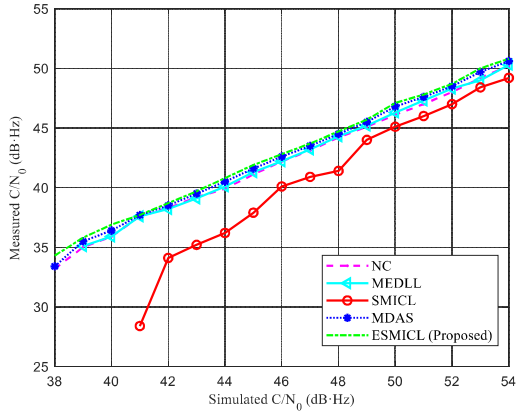

(c)

Fig. 8 (a) Means and (b) standard deviations of code errors, as well as (c)measured C/N0 of SMICL, MDAS, ESMICL, NC and MEDLL

C. Multipath Code Error Envelope

Multipath code error envelope can illustrate the influence of multipath with different delays on code loops. S-curves of ESMICLD and MoSMICLD both have a gap at the zero-crossing point that brings about an excessive adjustment towards positive values. Constant noise invokes constant positive fluctuation of code errors, which ultimately evolves into a positive bias. Therefore, for these two code loops, the upper and lower boundaries of multipath code error envelope appear when the gap (absolute value) reaches the maximum and minimum, respectively.

Fig. 9 exhibits multipath code error envelopes of the five loops, where the multipath delay varies from 0 to 1 chip. Except for the multipath delay and the difference of carrier phase between multipath and LOS, the other relevant parameters are shown in TABLE IV.

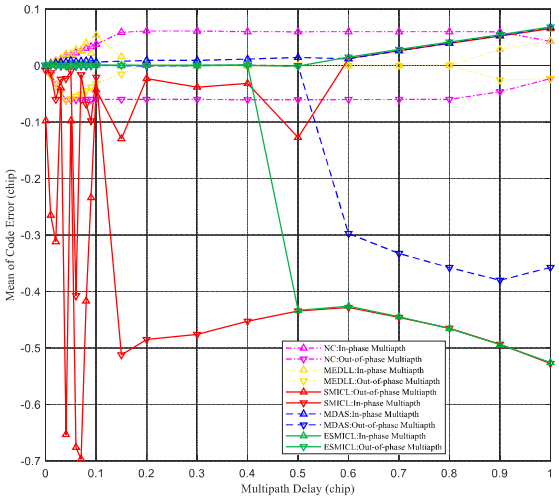

(a)

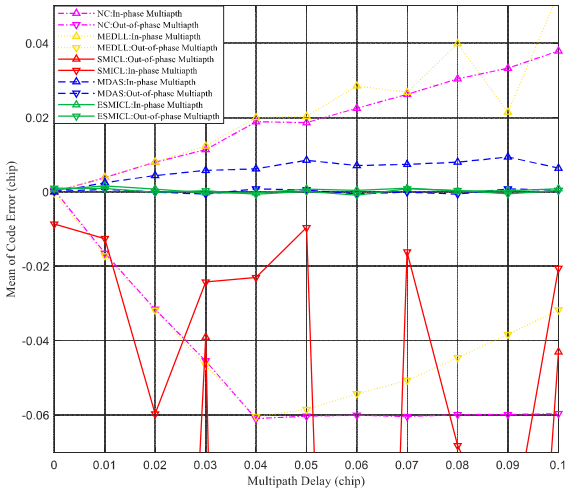

(b)

Fig. 9 Measured Multipath Code Error Envelopes for SMICL, MDAS, NC and MEDLL vs. the multipath delay of (a) [0, 1 chip] and (b) [0, 0.1 chip]

As shown in Fig. 9, when multipath delay is less than 0.5 chips, the upper and lower boundaries of ESMICL's multipath code errors correspond to out-of-phase and in-phase multipath, respectively. On the contrary, when multipath delay is larger than 0.5 chips, its upper and lower boundaries correspond to in-phase and out-of-phase multipath, respectively. The details

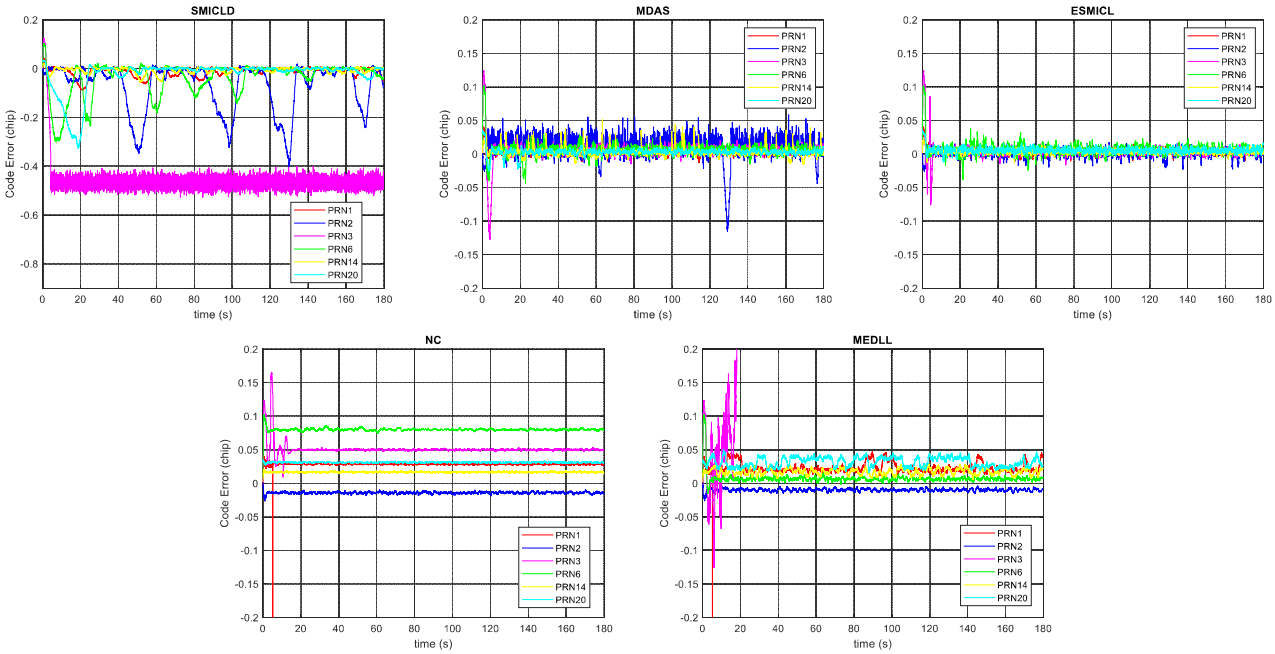

Fig. 10 Code errors of SMICL, MDAS, ESMICL, NC, and MEDLL in the IF-level software-based simulation

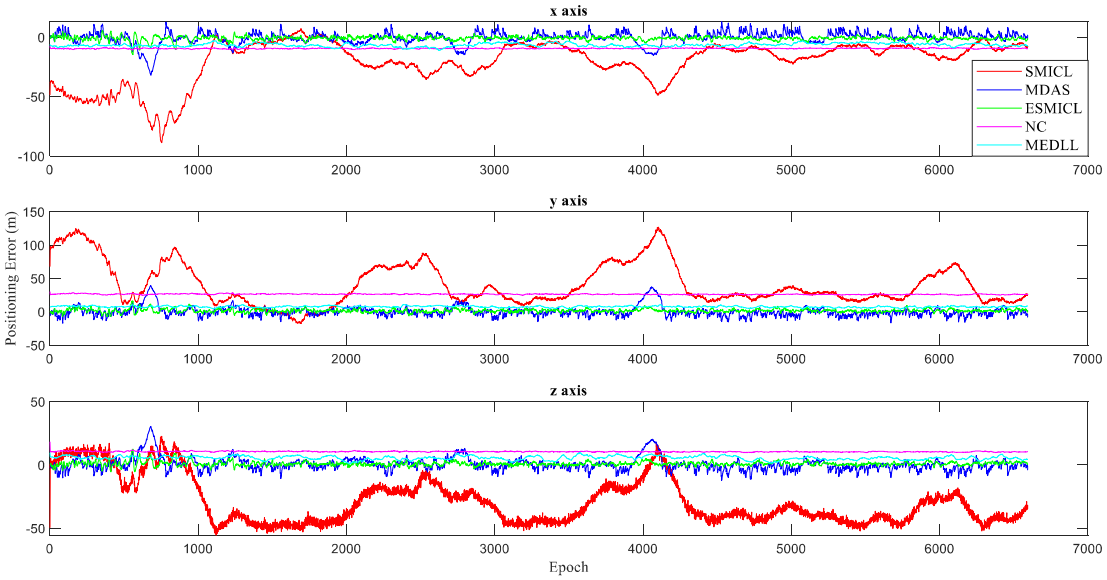

Fig. 11 Positioning errors of SMICL, MDAS, ESMICL, NC, and MEDLL in the IF-level software-based simulation

about the multipath code error envelope of MDAS can be found in [33].

Fig. 9 indicates that ESMICL can almost eliminate short multipath with delay of less than 0.5 chips, with the smallest code error mean of 10^{-4} orders of magnitude among these five code loops. Even though ESMICL is designed to deal with the multipath with the delay of larger than d ($\Delta/64 \approx 0.015$ chips), the test result shows that it still works when the multipath delay is 0.01 chips.

By contrast, the multipath code error envelope of SMICL fluctuates seriously towards negative direction, which conforms to the analysis before. In terms of MDAS, the upper boundary of the multipath code error envelope is about 0.01 chips because of the larger gap at the zero-crossing point of its S-curve. As it is well-known, NC cannot thoroughly eliminate the code error induced by multipath with any delay. MEDLL can mitigate medium and long multipath effectively but useless for short multipath whose delay is less than 0.18chips in this simulation test. Therefore, ESMICL has the best short multipath mitigation performance among these code loops. Nevertheless, when the multipath delay is larger than $\Delta/2$, SMICL does not work normally. ESMICL and Modified DLL Aided by DLL, which are based on SMICL, also have such weakness.

D. Positioning Errors

In this section, the positioning errors of ESMICL are compared with those of SMICL, MDAS, NC, and MEDLL. The positioning scene is simulated by our software-defined GPS IF signal simulator. The parameters of the simulated signal are displayed in TABLE VI. The C/N0 is set as 52 dB•Hz, which is consistent with the pre-measured C/N0 in a real indoor scene. Each PRN channel is influenced by a short multipath ray, the specific parameters of which are shown in TABLE VII.

TABLE VI
Parameters Used in the GPS RF signal simulator

Parameters	Values
Intermediate Frequency f_{IF}	75.42 MHz
Longitude	116° E
Latitude	40° N
Height	100 m

TABLE VII
MULTIPATH PARAMETERS

PRN	a_1	τ_1 (chip)	θ_0- θ_1
PRN1	0.4	0.1	$\pi/6$
PRN2	0.6	0.14	$3\pi/4$
PRN3	0.5	0.3	0
PRN6	0.8	0.2	π
PRN14	0.5	0.05	$\pi/3$
PRN20	0.8	0.07	0
PRN25	0.4	0.05	$3\pi/8$

GPS L1 C/A software receivers based on NC, MEDLL, SMICL, MDAS and ESMICL have been used to process the simulated signal. The configurations of these code loops are the same as before.

The code errors of the five code loops are shown in Fig. 11. The code errors of SMICL fluctuate seriously because SMICLD cannot adjust negative code errors promptly. For PRN3 satellite channel, the code error of SMICL even drifts in negative direction and eventually locks to a negative value. MDAS and ESMICL both have much smaller and more stable code errors than SMICL. But MDAS's code errors fluctuate towards the positive direction more severely than EMICL because of the larger gap at the zero point of the S-curve of its discriminator. NC and MEDLL cannot mitigate short multipath and both have certain code error biases for each PRN channel. Therefore, in accordance with the previous analysis in Section V, in terms of code errors, ESMICL has the best short multipath mitigation performance in noise environment.

The positioning results of these receivers are compared with the position coordinates set in the GPS IF signal simulator, from which the positioning errors are calculated. The positioning errors of the five code loops are exhibited in Fig. 12 and analyzed statistically in Fig. 12.

As shown in Fig. 12 and Fig. 12, ESMICL receiver has the smallest positioning errors on each axis among the five receivers. The positioning accuracy of ESMICL receiver reaches the decimeter level in the single short multipath scene. The specific comparison is given below.

Compared with SMICL, the positioning errors of x, y, and z axes of ESMICL have been reduced by more than 97%, 96% and 97%, respectively. Compared with MDAS, the positioning errors of x, y and z axes of ESMICL have been reduced by more than 63%, 37% and 57%, respectively. The means of ESMICL's x and z axis positioning errors are less than 1m.

Fig. 12 (b) shows that ESMICL also has the smallest standard deviation of positioning errors among the three code loops based on SMICLD, which means the anti-noise performance has been improved. However, because of the discontinuity at the zero-crossing point of its S-curve, the standard deviation of ESMICL is still larger than that of NC, which implies that ESMICL is more sensitive to noise than NC. But the anti-noise performance of ESMICL is close to MEDLL, and even better than MEDLL on x and y axes.

The main challenge of multipath mitigation techniques is to eliminate the positioning bias caused by multipath, while the standard deviation of positioning errors can be further reduced by filtering, smoothing and other existing denoising methods. Therefore, ESMICL outperforms other four code loops, considering both the short multipath mitigation performance and the anti-noise capability.

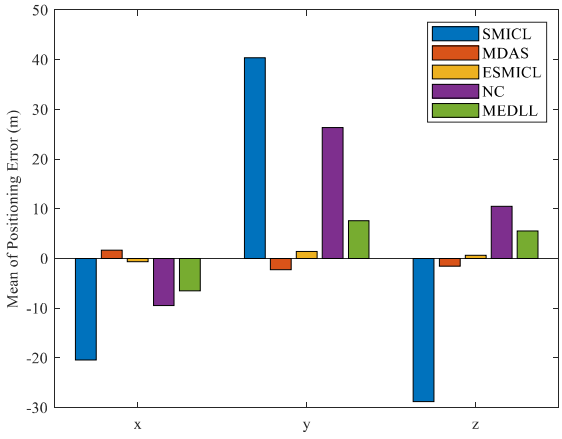

(a)

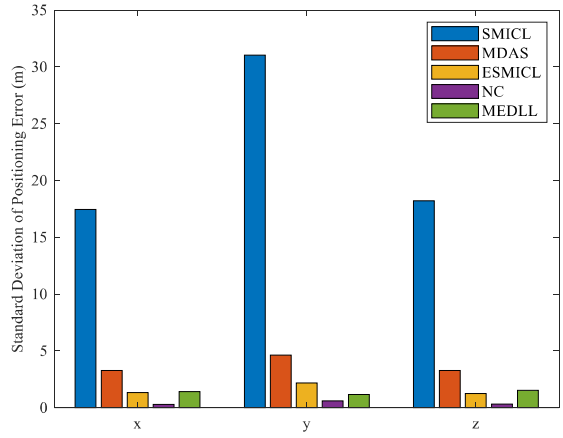

(b)

Fig. 12 Positioning errors of SMICL, MDAS, ESMICL, NC and MEDLL: (a) means of positioning errors of xyz-axes; (b) Standard deviations of positioning errors of xyz-axes

VI. Conclusion

By improving the S-curve of SMICLD, ESMICL proposed in this paper can be a practical solution to the problem of mitigating single short multipath with delay of less than 0.1chips (GPS L1 C/A, about 30 m), even less than 0.02 chips (GPS L1 C/A, about 6 m), in noise environment. ESMICL propels the SMICLD from the theory to practical applications. ESMICL can be used in the scene where single short multipath reflection exists, such as the road with buildings on single side.

However, ESMICL cannot mitigate multiple multipath rays robustly and have no effect on long multipath, the delay of which is generally larger than 0.5 chips (GPS L1 C/A, about 150 m). Solving these two problems will be a challenging topic in the future research.

VII. Appendix

To calculate the maximum discriminating value of SMICLD in the interval of [0 d] when the multipath delay exceeds d, we firstly study the expression of SMICLD. If $0 \le \varepsilon \le d < \tau_1 < \min(\Delta/2, 1-\Delta/2)$, SMICLD can be illustrated by an quadratic function

$$\begin{aligned} D(\varepsilon) &= 2a_0^2(2-\Delta)\varepsilon \\ &\quad + 4a_0a_1\cos(\theta_0-\theta_1)\varepsilon(1+\varepsilon-\tau_1-\frac{\Delta}{2}) \\ &= 4a_0a_1\cos(\theta_0-\theta_1)\varepsilon^2 \\ &\quad + \left[2a_0^2(2-\Delta)+4a_0a_1\cos(\theta_0-\theta_1)(1-\tau_1-\frac{\Delta}{2})\right]\varepsilon \end{aligned} \tag{A1}$$

The axis of symmetry of this parabola is located at ε_s, which can be expressed as

$$\varepsilon_s = -\frac{a_0(2-\Delta)+a_1(2-\Delta-2\tau_1)\cos(\theta_0-\theta_1)}{4a_1\cos(\theta_0-\theta_1)} \tag{A2}$$

A. If $\cos(\theta_0-\theta_1) > 0$, the maximum value of SMICLD can be calculated as $D(d)$

$$D(d) = 4a_0d\left[a_1\left(1-\tau_1+d-\frac{\Delta}{2}\right)\cos(\theta_0-\theta_1)+a_0\left(1-\frac{\Delta}{2}\right)\right] \tag{A3}$$

Providing that $a_0 = 1$, $a_1 \le 1$, $0 \le \cos(\theta_0-\theta_1) \le 1$, the upper bound of $D(d)$ can be written as

$$D(d) \le 4d(2-\tau_1-\Delta+d) \tag{A4}$$

B. If $\cos(\theta_0-\theta_1) < 0$, the maximum value of SMICLD may be $D(d)$ or $D(\varepsilon_s)$, which depends on whether the axis of symmetry is in the interval of [0 d]. When the axis of symmetry is out of [0 d], the maximum value of SMICLD is $D(d)$, the same as case A. In the other situation, the maximum of SMICLD is given by

$$D(\varepsilon_s) = -\frac{4a_0\left[a_0(2-\Delta)+a_1(2-\Delta-2\tau_1)\cos(\theta_0-\theta_1)\right]^2}{16a_1\cos(\theta_0-\theta_1)} \tag{A5}$$

In this respect, ε_s is within d, from which we can get

$$0 < a_0(2-\Delta)+a_1(2-\Delta-2\tau_1)\cos(\theta_0-\theta_1) < -4a_1d\cos(\theta_0-\theta_1) \tag{A6}$$

Combining the condition of $a_0 = 1$, $a_1 \le 1$, $-1 \le \cos(\theta_0-\theta_1) \le 0$, we can get the upper limit to $D(\varepsilon_s)$ as follows

$$D(\varepsilon_s) < 4d^2 \tag{A7}$$

Given the multipath delay is less than min ($\Delta/2$, $1-\Delta/2$), the following relationships can be get easily

$$D(\varepsilon_s) < 4d^2 < 4d(2-\Delta-\tau_1+d) \tag{A8}$$

To conclude, the maximum value of SMICLD in the interval of [0 d] is given by

$$D^{max}(\varepsilon) = 4d(2-\Delta-\tau_1+d) \tag{A9}$$

Considering $d < \tau_1$,

$$D^{max}(\varepsilon) \le 4d(2-\Delta) \tag{A10}$$

If the spacing of multi-correlators d is equal to $\Delta/64$, the maximum value is computed as follows

$$D^{max}_{d=\Delta/64}(\varepsilon) = (2\text{-}\Delta)\bullet\frac{\Delta}{16} \tag{A11}$$

VIII. Reference

[1] Y. Luo, Z. Weng, *et al*., "Short-Baseline High-Precision DGPS for Smart Snow Blower," *IEEE Internet of Things Journal*., to be published. DOI: 10.1109/JIOT.2020.2972746.

[2] Z. Fang, C. Ma, X. Wang, J. Qu and S. Zhang, "Identify individuals behaviors based GPS trajectories in the Internet of Things," *2016 First IEEE International Conference on Computer Communication and the Internet (ICCCI)*, Wuhan, 2016, pp. 384-387.

[3] S. M. Alzahrani, "Sensing for the Internet of Things and Its Applications," *2017 5th International Conference on Future Internet of Things and Cloud Workshops (FiCloudW)*, Prague, 2017, pp. 88-92.

[4] S. Shen, Z. Wei, L. Sun, *et al*., "The Shared Bicycle and Its Network-Internet of Shared Bicycle (IoSB): A Review and Survey," *Sensors (Basel)*., 18(8):2581, Aug. 2018.

[5] S. Kuutti, S. Fallah, K. Katsaros, M. Dianati, F. Mccullough and A. Mouzakitis, "A Survey of the State-of-the-Art Localization Techniques and Their Potentials for Autonomous Vehicle Applications," *IEEE Internet of Things Journal*, vol. 5, no. 2, pp. 829-846, Apr. 2018.

[6] H. Lee, J. Wang, C. Rizos, et al., "GPS/Pseudolite/INS integration: concept and first tests," *GPS Solutions* 6, pp. 34–46, Nov. 2002.

[7] K. Larson, D. Akos and L. Marti, "Characterizing Multipath from Satellite Navigation Measurements in Urban Environments," *2008 5th IEEE Consumer Communications and Networking Conference*, Las Vegas, NV, 2008, pp. 620-625.

[8] A. Rusu- Casandra, I. Marghescu and E. S. Lohan, "Estimators of the indoor channel for GPS-based pseudolite signal," *2010 9th International Symposium on Electronics and Telecommunications*, Timisoara, 2010, pp. 233-236.

[9] L. R. Weill, "Conquering mutlipath: The GPS accuracy battle," *GPS World*, 1997, 4, pp. 59-66.

[10] M. S. Grewal, L. R. Weill, *et al*., Global positioning systems, inertial navigation, and integration. New York, NY, USA: John Wiley & Sons, Inc., 2001.

[11] C. C. Counselman, "Multipath-rejecting GPS antennas," in *Proceedings of the IEEE*, vol. 87, no. 1, pp. 86-91, Jan. 1999.

[12] F. Scire-Scappuzzo and S. N. Makarov, "A Low-Multipath Wideband GPS Antenna With Cutoff or Non-Cutoff Corrugated Ground Plane," *IEEE Transactions on Antennas and Propagation*, vol. 57, no. 1, pp. 33-46, Jan. 2009.

[13] L. R. Weill, "Multipath Mitigation Using Modernized GPS Signals: How Good Can it Get?," in *Proc. ION ITM*, Portland, OR, USA, 2002, pp. 493-505.

[14] Method for mitigating multipath effects in radio systems, by L. R. Weill, B. Fisher. (2002, Apr., 9). Patent 6370207. [Online]. Available: http://www.freepatentsonline.com/6031881.html

[15] R. D. J. Van Nee, "The Multipath Estimating Delay Lock Loop," in *Proc. IEEE 2nd Int. Symposium on Spread Spectrum Techniques and Applications*, Yokohama, Japan, 1992, pp. 39-42.

[16] X. Chen, F. Dovis, *et al*., "Comparative studies of GPS multipath mitigation methods performance," *IEEE Trans. on Aerospace & Electronic Systems*, 2013, 49(3), pp. 1555-1568.

[17] A. J. V. Dierendonck, P. Fenton and T. Ford, "Theory and Performance of Narrow Correlator Spacing in a GPS Receiver," *Navigation*, vol. 39, no. 3, 1992, pp. 265-284.

[18] B. Townsend, P. Fenton, "A practical approach to the reduction of pseudorange multipath errors in a L1 GPS receiver," in *Proceedings of the*

7th International Technical Meeting of the Satellite Division of the Institute of Navigation, Salt Lake City, UT, USA. 1994, pp. 20-23.
[19] L. Garin, J. M. Rousseau, "Enhanced Strobe Correlator Multipath Rejection for Code & Carrier," in *Proc. ION ITM*, Kansas City, MO, USA, 1997, pp. 559-568.
[20] High Resolution Correlator Technique for Spread Spectrum Ranging System Code and Carrier Multipath Mitigation, by G.A. Mcgraw. (2004, Feb., 3). Patent 6687316, [Online]. Available: http://www.freepatentsonline.com/6687316.html
[21] J. M. Sleewaegen, F. Boon, "Mitigating short-delay multipath: a promising new technique," in *Proc. ION GPS*, Salt Lake City, UT, USA, 2001, pp. 11-14.
[22] M. Z. H. Bhuiyan, E. S. Lohan and M. Renfors, "A Slope-Based Multipath Estimation Technique for Mitigating Short-Delay Multipath in GNSS Receivers," in *Proc. IEEE Int. Symposium on Circuits and Systems*, Paris, France, 2010, pp. 3573-3576.
[23] Y. Gao, Q. Li, "Modified Narrow Correlator Spacing Method for Mitigation Short-Delay Multipath," *Measurement and Control Technology*, 2014, 33(1), pp. 43-46.
[24] Z. Zhang, C. L. Law, "Short-delay Multipath Mitigation Technique Based on Virtual Multipath," *IEEE Antennas & Wireless Propagation Letters*, 2005, 4, pp. 344-348.
[25] F. Zhou, S. Huang, "Multi-Path Mitigation Based on Teager-Keiser Operator," *Journal of University of Electronic Science and Technology of China*, 2007, 36(4), pp. 692-695.
[26] J. MO, Z. Deng, B. Jia, *et al*., "A Novel Multipath Mitigation Method Based on Fast Orthogonal Search (FOS) for Short-Delay Multipath with Zero Doppler Shift Difference," in *Proc. CSNC*, Harbin, China, 2018, pp. 289-299.
[27] R. D. J. Van Nee, J. Siereveld, *et al.*, "The Multipath Estimating Delay Lock Loop: Approaching Theoretical Accuracy Limits," in *Proc. IEEE Position Location and Navigation Symposium*, Las Vegas, NV, USA, 1994, pp. 246-251.
[28] R. D. J. Van Nee, "Multipath and multi-transmitter interference in spread-spectrum communication and navigation systems," Ph.D. dissertation, Dept. Elect. Eng., TU Delft, Delft, Netherlands, 1995.
[29] N. Jardak, N. Samama, "Short Multipath Insensitive Code Loop Discriminator," *IEEE Transactions on Aerospace and Electronic Systems*, 2010, 46(1), pp. 278-295.
[30] A. I. Mustafa, S. S. El-Sheikh, *et al.*, "Modified short multipath insensitive code loop discriminator," in *Proc. IEEE Int. Conf. on INFOS*, Cairo, Egypt, 2012, pp. NW-60-NW-67.
[31] E. S. Hassan, A. I. Mustafa, K. H. Awadalla, *et al*., "A New Modified Short-Multipath-Insensitive Code Loop Discriminator," *Wireless Personal Communications*, 2018, pp. 1-17.
[32] X. Weng, Y. Kou, "Modified Code Tracking Loop Aided by Short Multipath Insensitive Code Loop Discriminator," in *Proc. ION ITM*, Monterey, CA, USA, 2017, pp. 1316-1329.
[33] X. Weng, Y. Kou, "Modified Delay Lock Loop Aided by Short Multipath Insensitive Code Loop Discriminator," *Navigation*, to be published.
[34] N. Jardak, A. Vervisch-Picois and N. Samama, "Multipath Insensitive Delay Lock Loop in GNSS Receivers," *IEEE Transactions on Aerospace and Electronic Systems*, vol. 47, no. 4, pp. 2590-2609, Oct. 2011.
[35] B. B. W. Parkinson, J. J. Spilker, *et al.,* Global Positioning System: Theory and Applications, volume 1. Washington DC, USA: American Institute of Aeronautics and Astronautics, 1996.
[36] E. D. Kaplan, C. Hegarty, Understanding GPS: Principles and Applications, 2nd ed. Norwood, MA, USA: Artech House, 2006.

Xu Weng was born in Xuzhou, Jiangsu, China in 1993. He received the B.S. degree in electrical engineering from Nanjing University of Aeronautics and Astronautics, Nanjing, China, in 2015 and the M.S. degree in electrical engineering from Beihang University, Beijing, China, in 2018.

Yanhong Kou received her Ph.D. degree in communication and information systems from Beihang University, China in 2006, the M.S. degree in communication and electronic systems from the University of Electronic Science and Technology of China in 1996, and the B.S. degree in radio physics from Sichuan University, China in 1991.

She was a postdoctoral research fellow at Miami University from 2009 to 2010. She has been an associate professor in School of Electronics and Information Engineering at Beihang University since 2003. She is the author of 1 book and more than 100 articles. Her research interests include high-performance GNSS receivers and signal simulators, signal processing in degraded conditions, and satellite navigation and communication systems. She holds 13 patents and has chaired more than 10 sessions for international conferences.